energies

MDPI

Article

Thermal Perturbations at Crystal Nucleation in Glass-Forming Liquids

Alexander Minakov [1] and Christoph Schick [2,*]

[1] Prokhorov General Physics Institute of the Russian Academy of Sciences, Vavilov Str. 38, 119991 Moscow, Russia
[2] Institute of Physics and Competence Centre °CALOR, University of Rostock, Albert-Einstein-Str. 23-24, 18051 Rostock, Germany
* Correspondence: christoph.schick@uni-rostock.de

Abstract: Understanding the processes occurring during the nanocrystallization of glass-forming liquids is important for creating artificial nanostructures for various applications. In this article, local thermal perturbations in supercooled glass-forming liquids and polymers during the nucleation of a crystalline phase are studied. To describe the thermal response of supercooled glass-forming liquids, an integro-differential heat equation with dynamic heat capacity is used. We have found that the effect of the dynamic heat capacity is significant for fast local thermal perturbations that arise in the early stages of crystal nucleation in glass-forming liquids and polymers. It has been established that local temperature perturbations during the nucleation of crystals in silicate glasses and polymers can change the nucleation rate by 2–5 orders of magnitude. The knowledge gained can be useful for the technology of artificial microstructures and advanced materials.

Keywords: nonequilibrium heat transfer; phase transitions; crystallization; glass-forming liquids; dynamic heat capacity

Citation: Minakov, A.; Schick, C. Thermal Perturbations at Crystal Nucleation in Glass-Forming Liquids. *Energies* **2022**, *15*, 9005. https://doi.org/10.3390/en15239005

Academic Editors: Pavel Skripov and Aleksandr Pavlenko

Received: 1 November 2022
Accepted: 24 November 2022
Published: 28 November 2022

1. Introduction

This work is devoted to the problem of heat transfer, which is associated with nonequilibrium thermal processes in metastable liquids. In this study, we are interested in nonequilibrium heat transfer in undercooled glass-forming liquids, in which the process of the early stages of crystal nucleation occurs at the nanoscale. Glasses and polymers are often used to develop new advanced nanocrystalline materials and composites. The properties of glass-forming materials can be varied over a wide range by controlling the crystallization process with appropriate heat treatments, without changing the composition. Glass-forming materials are materials that form glasses at relatively moderate cooling rates (i.e., do not require extreme quenching). Accordingly, the glass-forming liquid is a liquid melt of the glass-forming material. Various artificial nanostructures can be created using the controlled crystallization of glass-forming liquids; this fact is used in many applications, such as additive manufacturing [1–4]. The fields of application of glass-forming materials can be greatly extended using optimal annealing treatments [5]. Thus, by the appropriate annealing of glass-forming materials, a mixed glassy-nanocrystalline structure can be obtained [5,6]. Nanosized crystalline particles, selectively introduced into the glass matrix, can significantly improve the mechanical properties of glasses. For example, the mechanical properties of aluminum-based glasses have been significantly improved by selectively introducing nanosized crystalline particles into the glass matrix [7–9]. In addition, an artificially created microstructure can be used to increase the kinetic stability of such nanoglasses [5,6]. In addition, understanding the behavior of subcritical nuclei is important for developing advanced materials for phase-change memory devices [10]. Indeed, the role of the crystallization process is very important in laser memory devices with a melting–crystallization phase transition. A phase-change material should have as fine a nanostructure as possible.

In addition, it should neither be too difficult to crystallize (because it would require excessive power or conversion time) nor crystallize too easily (because it would compromise long-term data storage by initiating unwanted crystallization) [10]. In fact, subcritical nuclei are constantly developing and decaying. Only near-critical nuclei can commonly reach the critical size and grow into stable crystal grains (note that a small local change in temperature can significantly affect the dynamics of near-critical nuclei). Experimental studies of the early stages of crystallization are challenging due to the nanometer size and the very short lifetime of subcritical and near-critical nuclei. However, the nucleation of crystals can often be studied at low supercooling, and at very high supercooling, near the glass transition temperature, and in the case of liquids with low crystal-growth rates, even over the entire supercooling range from the melting temperature to the glass transition temperature [11]. Thus, developing new promising nanocrystalline glass-forming materials requires a deep understanding of the kinetics of the early stages of crystal nucleation. In fact, the formation of nanocrystallized materials is commonly associated with homogeneous nucleation [12–15]. In this paper, we will focus on homogeneous nucleation in glass-forming liquids above the glass transition temperature, T_g.

Local temperature changes associated with the energetics of nuclei formation can significantly affect nucleation dynamics. In this article, we study the influence of the local temperature perturbations $\delta T(t, r)$ associated with the nucleation of crystals on the processes of the early stage of nucleation in glass-forming liquids. We will not consider crystal precursors in undercooled liquids [16,17]. Thus, we consider homogeneous nucleation which is not affected by pre-existing clusters. The scenario of two-stage nucleation, which can occur due to the formation of precursors, can be considered in a separate article. Here, our goal is to study the effect of local temperature perturbations $\delta T(t, r)$ associated with crystal nucleation on the formation of nuclei in glass-forming liquids, and to study heat transfer processes at the stage of crystal nucleation. Note also that the local temperature distribution was considered for the non-isothermal homogeneous nucleation of water vapor under quasi-isothermal conditions in [18]. Here, we are interested in the local temperature change during nucleation in condensed matter. In addition, we consider the effect of dynamic heat capacity relaxation on the heat transfer at this stage of nucleation.

The dynamic heat capacity $c_{dyn}(t)$ of glass-forming liquids and polymers as a function of time t (or frequency) has been intensively studied since the pioneering work of Birge and Nagel [19]. For example, see heat capacity spectroscopy in polymers [20,21]. The time dependence $c_{dyn}(t)$ is associated with slow energy exchange between different degrees of freedom in glass-forming liquids and polymers. Because $c_{dyn}(t)$ is time-dependent, the local change in temperature over time depends on the temperature distribution in these liquids at earlier times. This behavior can be described using the integro-differential heat equation with "memory" [22]. The influence of the dynamic heat capacity $c_{dyn}(t)$ is most significant for fast local thermal perturbations on the nanometer scale [22]. This work aims to determine the local thermal perturbations $\delta T(t, r)$ (associated with the nucleation of crystals) and the effect of these perturbations on the nucleation rate $I(T)$ in glass-forming liquids.

The first part of the article considers the influence of a local temperature change on the nucleation rate in silicate glasses and polymers. In the second part, the influence of the dynamic heat capacity $c_{dyn}(t)$ on thermal perturbations in glass-forming liquids is estimated. An analytical solution of the integro-differential heat equation with dynamic heat capacity $c_{dyn}(t)$ is constructed for a spherically symmetric problem. In fact, we consider a simple model of creation and decay of a spherical nucleus under spherically symmetric boundary conditions. Finally, local temperature perturbations during the nucleation and decay of crystalline nuclei in silicate glasses and polymers are considered.

2. Crystal Nucleation in Glass-Forming Liquids

Isothermal processes are considered in the classical theory of homogeneous nucleation [23–27]. This consideration is justified for materials with moderate and high thermal

conductivity. However, glass-forming liquids, especially polymers, can have a low thermal conductivity λ of the order of 0.1 W/m·K [28]. For this reason, local temperature changes associated with the nucleation process can be significant on the nanosecond time scale (see below). In addition, the nonequilibrium thermal response of glasses and polymers is associated with the relaxation of the dynamic heat capacity, which can significantly affect local thermal perturbations in these substances during crystal nucleation [22,29]. Note also that the pre-exponential factor I_0 of the rate of homogeneous nucleation, measured in many experiments, significantly exceeds the theoretical value [12,13,30,31]. The discrepancy between the experimental and theoretical values of the pre-exponential factor I_0 can possibly be reduced by taking into account the temperature dependence of the interfacial free energy σ [13] and seeded crystallization [31,32]. In this article, we explore an additional cause that can affect the rate of nucleation.

The probability of a thermodynamic fluctuation creating a crystal nucleus is proportional to $\exp(-R_{min}/k_BT)$, where k_B is Boltzmann's constant, and R_{min} is the minimum work required to create a nucleus [23,24]. A local pressure perturbation associated with a thermodynamic fluctuation of radius r relaxes on a time scale of the order of r/V_{sound}, where the speed of sound V_{sound} is about several thousand m/s. Thus, the local pressure relaxes on a picosecond scale at r of the order of several nm or fewer. Therefore, the local pressure near such fluctuations can be considered constant on a nanosecond time scale. The time required for the formation of a crystalline nucleus from the beginning of its formation is denoted by τ_f. This formation time τ_f should not be confused with the induction time and the time lag before the beginning of the formation of crystal nuclei (for example, in molecular dynamics simulations). Usually, the time lag before the beginning of the formation of crystal nuclei is much longer than τ_f [33]. In fact, the formation of crystal nuclei with a size of the order of 1 nm in various materials can occur over a time in the range of 0.01–1 ns [4,33–38], and in polymers, τ_f can vary on the nanosecond scale [39–43].

For a spherical nucleus, R_{min} is equal to the Gibbs free energy

$$\Delta G(r) = 4\pi\sigma r^2 - 4\pi r^3 \Delta g_v/3, \quad (1)$$

required for the creation of a nucleus of radius r, where σ is the solid/liquid interfacial energy, $\Delta g_v = \Delta h_m \Delta T/T_{m0}$ is the change in volumetric Gibbs free energy at crystallization, Δh_m is the volumetric enthalpy of melting, T_{m0} is the equilibrium melting temperature, and $\Delta T = (T_{m0} - T)$ is undercooling [12,23–27,44]. Furthermore, we will consider critical and subcritical nuclei with $r \le r_C$, where the critical radius $r_C = 2\sigma/\Delta g_v$ corresponds to the energy barrier for homogeneous nucleation $\Delta G_C = \frac{16\pi\sigma^3}{3\Delta g_v{}^2}$, or $\Delta G_C = \frac{2\pi\Delta g_v r_C^3}{3}$ [12,23–27]. Therefore, $\Delta G_C = V_C\Delta g_v/2$, where $V_C = 4\pi r_C^3/3$ is the volume of the critical nucleus.

In the case of polymers, the Gibbs free energy required for the formation of a lamellar nucleus with thickness l and radius r is equal to

$$\Delta G(l,r) = 2\pi r^2\sigma_e + 2\pi rl\sigma - \pi r^2 l\Delta g_v, \quad (2)$$

where σ_e and σ correspond to the surface free energy of the lamellar basal plane (fold surface) and the lateral (side) interface, respectively [13,16]. The approximate free-energy difference $\Delta g_v = \Delta h_m\Delta T/T_{m0}$ between the liquid and crystal can be corrected and presented as $\Delta g_v = \Delta h_m\left(\frac{\Delta T}{T_{m0}}\right)\left(\frac{T}{T_{m0}}\right)$ (which is often used for polymers [13]), or even $\Delta g_v = \Delta h_m\left(\frac{\Delta T}{T_{m0}}\right)\left(\frac{7T}{T_{m0}+6T}\right)$ [44]. However, these corrections are not significant for the present study, since our estimates do not claim to be highly accurate. Thus, we will consider the following approximation: $\Delta g_v = \Delta h_m\Delta T/T_{m0}$. In this case, the critical radius $r_C = 2\sigma/\Delta g_v$ and critical thickness $l_C = 4\sigma_e/\Delta g_v$ are associated with the energy barrier for homogeneous nucleation $\Delta G_C = \frac{8\pi\sigma^2\sigma_e}{\Delta g_v{}^2}$ [13,16]. Therefore, $\Delta G_C = V_C\Delta g_v/2$, where $V_C = \pi r_C^2 l_C$ is the volume of the critical nucleus.

The nucleus of the solid phase, created due to thermodynamic fluctuations, has additional energy compared to the metastable initial liquid phase. The energy $\Delta G(r)$ spent on the creation of the nucleus is compensated by the local cooling of the material at the site of the nucleus. This local change in temperature δT, associated with the energy required for the formation of nuclei, can significantly affect the dynamics of the nucleation and evolution of nuclei. In fact, a significant number of unstable nuclei (with $r < r_C$) can be transformed into stable nuclei (with $r \geq r_C$), since the critical radius $r_C = 2\sigma T_{m0}/\Delta h_m(T_{m0} - T)$ decreases with decreasing the local temperature T. We will focus on local fast thermal perturbations in glass-forming liquids above the glass transition temperature T_g. Therefore, we will not consider the effect of long-term structural relaxation, which is noticeable near and below T_g, on the nucleation dynamics [45–48]. However, we consider the effect associated with the dynamic heat capacity, which is significant for fast local thermal perturbations in glass-forming liquids, even well above the glass transition temperature T_g [22,29].

2.1. Influence of Local Temperature Change on the Nucleation Rate $I(T)$ in Silicate Glasses

The local change in temperature δT associated with the energy required for the formation of nuclei can be about 1 K (see below). In this case, the evolution of near-critical nuclei and the nucleation rate $I(T)$ can change significantly. In fact, the nucleation rate $I(T)$ is proportional to $\exp\left(-\frac{\Delta G_C}{k_B T}\right)$ [12,13,23–27]. The relative increase in the rate is equal to

$$\frac{I(T+\delta T)}{I(T)} = \exp\left(-\frac{\Delta G_C}{k_B T}\cdot\frac{2\delta T}{\Delta T}\right), \quad (3)$$

at $|\delta T| \ll \Delta T$ (an insignificant value of $\frac{\delta T}{T}$ compared to $\frac{2\delta T}{\Delta T}$ is neglected). Table 1 shows the influence of the thermal perturbation δT on the relative change in the rate of nucleation $\frac{I(T+\delta T)}{I(T)}$ at $\delta T = -1$ K for silicate glasses. The parameters of the silicate glasses are known from the literature [12,49–53].

Table 1. Relative increase in the nucleation rate $\frac{I(T+\delta T)}{I(T)}$ in silicate glasses at $\delta T = -1$ K.

Substance	Δh_m J/m^3	T_{m0} K	T K	ΔT K	σ J/m^2	Δg_v J/m^3	ΔG_C J	$\frac{\Delta G_C}{k_B T}$	$\frac{I(T+\delta T)}{I(T)}$
$Li_2O{\cdot}2SiO_2$	9.4×10^8	1310	1160	150	0.20	11.0×10^7	1.17×10^{-17}	728	1.65×10^4
$Na_2O{\cdot}2CaO{\cdot}3SiO_2$	7.2×10^8	1560	1360	200	0.19	9.23×10^7	1.35×10^{-17}	718	1.32×10^3
$2Na_2O{\cdot}CaO{\cdot}3SiO_2$	4.97×10^8	1448	1248	200	0.17	6.86×10^7	1.75×10^{-17}	1013	2.25×10^4
$BaO{\cdot}2SiO_2$	5.11×10^8	1690	1490	200	0.13	6.05×10^7	1.0×10^{-17}	488	1.32×10^2

Next, we estimate the effect of the kinetic barrier on the nucleation rate $I(T)$ under thermal perturbations δT in silicate glasses. In fact,

$$I(T) = I_0 exp\left(-\frac{\Delta G_C}{k_B T}\right) exp\left(-\frac{\Delta G_D}{k_B T}\right), \quad (4)$$

where ΔG_D is the kinetic barrier to nucleation [49,50]. The kinetic barrier ΔG_D can be estimated from the activation free energy ΔG_η for a viscous flow [49,50]. Then,

$$I(T) = I_0 exp\left(-\frac{\Delta G_C}{k_B T}\right) exp\left(-\frac{B}{(T - T_0)}\right), \quad (5)$$

since the viscosity $\eta(T)$ usually obeys the Vogel–Fulcher–Tammann–Hesse (VFTH) equation [52,53].

$$log_{10}\eta = A + \frac{B}{(T - T_0)}. \quad (6)$$

Thus,

$$\frac{I(T+\delta T)}{I(T)} = A_{kin} exp\left(-\frac{\Delta G_C}{k_B T}\cdot\frac{2\delta T}{\Delta T}\right), \quad (7)$$

where

$$A_{kin} = exp\left(\frac{B}{(T-T_0)}\cdot\frac{\delta T}{(T-T_0)}\right). \quad (8)$$

Table 2 shows the influence of the thermal perturbation δT on the relative change in the rate of nucleation due to a change in the kinetic barrier at $\delta T = -1$ K for silicate glasses. The parameters of the silicate glasses are known from the literature [52,53].

Table 2. Relative change in the nucleation rate due to a change in the kinetic barrier in silicate glasses at $\delta T = -1$ K.

Substance	B **K**	T_0 **K**	T **K**	$T-T_0$ **K**	$B/(T-T_0)$ **-**	A_{kin} **-**
$Li_2O{\cdot}2SiO_2$	1347	595	1160	565	2.38	0.996
$Na_2O{\cdot}2CaO{\cdot}3SiO_2$	4893	547	1360	813	6.02	0.993
$BaO{\cdot}2SiO_2$	1702	795	1490	695	2.45	0.997

Thus, the effect of the kinetic barrier on the nucleation rate $I(T)$ at small temperature perturbations in silicate glasses is insignificant. However, thermal perturbations δT of the order of 1 K change the nucleation rate by 2–4 orders of magnitude (see Table 1), which is significant.

2.2. Influence of Local Temperature Change on the Nucleation Rate $I(T)$ in Polymers

The relative change in the rate of nucleation for glass-forming polymers is equal to $\exp\left(-\frac{\Delta G_C}{k_B T}\cdot\frac{2\delta T}{\Delta T}\right)$ at $|\delta T| \ll \Delta T$(see Equation (3)), where $\Delta G_C = \frac{8\pi\sigma^2\sigma_e}{\Delta g_v{}^2}$. As mentioned above, the small value of $\frac{\delta T}{T}$ compared to $\frac{2\delta T}{\Delta T}$ is neglected. Tables 3 and 4 show the influence of the thermal perturbation on the relative change in the rate of nucleation for polyethylene (PE) and isotactic polystyrene (iPS) at $\delta T = -0.5$ K (see Table 3), as well as polybutylene succinate (PBS) and isotactic polypropylene (iPP) at $\delta T = -1$ K (see Table 4). Temperature perturbations $\delta T = -0.5$ K (for PE and iPS) and $\delta T = -1$ K (for PBS and iPP) were evaluated as described below. The parameters of the polymers are known from the literature [13,54–60].

Table 3. Relative increase in the nucleation rate $\frac{I(T+\delta T)}{I(T)}$ in PE and iPS at $\delta T = -0.5$ K.

Polymer	Δh_m **J/m^3**	T_{m0} **K**	T **K**	ΔT **K**	σ_e **J/m^2**	σ **J/m^2**	Δg_v **J/m^3**	ΔG_C **J**	$\frac{\Delta G_C}{k_B T}$	$\frac{I(T+\delta T)}{I(T)}$
PE	2.8×10^8	418	388	30	0.093	0.0146	2.0×10^7	1.2×10^{-18}	230	2.2×10^3
iPS	9.1×10^7	516	486	30	0.035	0.0077	5.3×10^6	1.9×10^{-18}	278	1.1×10^4

Table 4. Relative increase in the nucleation rate $\frac{I(T+\delta T)}{I(T)}$ in PBS and iPP at $\delta T = -1$ K.

Polymer	Δh_m **J/m^3**	T_{m0} **K**	T **K**	ΔT **K**	σ_e **J/m^2**	σ **J/m^2**	Δg_v **J/m^3**	ΔG_C **J**	$\frac{\Delta G_C}{k_B T}$	$\frac{I(T+\delta T)}{I(T)}$
PBS	1.47×10^8	403	343	60	0.0337	0.0309	2.2×10^7	1.7×10^{-18}	354	1.3×10^5
iPP	1.57×10^8	461	421	40	0.07	0.0115	1.4×10^7	1.3×10^{-18}	216	5.0×10^4

The influence of the kinetic barrier on the nucleation rate $I(T)$ under thermal perturbations in polymers can be estimated as follows. The relative change in the rate of nucleation is equal to $A_{kin} exp\left(-\frac{\Delta G_C}{k_B T}\cdot\frac{2\delta T}{\Delta T}\right)$ (see Equation (7)), where A_{kin} is equal to $exp\left(\frac{B}{(T-T_0)}\cdot\frac{\delta T}{(T-T_0)}\right)$

(see Equation (8)), and $B = E_A/R$ depends on the diffusional activation energy E_A for the transport of polymer chain segments at the interface in polymers [13]; $R = 8.314$ J/mol·K is the universal gas constant [28], and usually, $E_A = 6.27$ kJ/mol and $T_0 \approx T_g - 30K$ [13]. The effect of the kinetic barrier on the nucleation rate under thermal perturbations in polymers is presented in Tables 5 and 6. The parameters of the polymers are known from the literature [13,54–58].

Table 5. Relative change in the nucleation rate due to a change in the kinetic barrier in PE and iPS at $\delta T = -0.5$ K.

Polymer	B K	T_0 K	T K	$T-T_0$ K	$B/(T-T_0)$ -	A_{kin} -
PE	754	118	388	270	2.79	0.995
iPS	754	330	486	156	2.29	0.985

Table 6. Relative change in the nucleation rate due to a change in the kinetic barrier in PBS and iPP at $\delta T = -1$ K.

Polymer	B K	T_0 K	T K	$T-T_0$ K	$B/(T-T_0)$ -	A_{kin} -
PBS	754	206	343	137	5.5	0.961
iPP	754	225	421	196	3.85	0.981

Thus, the effect of the kinetic barrier on the nucleation rate $I(T)$ at small temperature perturbations is again insignificant. However, thermal perturbations δT of the order of 1 K significantly change the nucleation rate in polymers by 3–5 orders of magnitude, as shown in Tables 3 and 4.

3. Thermal Perturbations in Glass-Forming Liquids

Next, we consider heat transfer processes in glass-forming liquids in order to determine the magnitude of thermal perturbations during the nucleation and decay of crystal nuclei. Since we are interested in thermal perturbations on a nanosecond time scale, it is necessary to take into account the influence of the dynamic heat capacity $c_{dyn}(t)$ of glass-forming liquids. For a spherically symmetric problem with zero initial conditions, the thermal response in glass-forming liquids can be described by the following integro-differential heat equation [22,29]:

$$\frac{\partial}{\partial t}\int_0^t \rho c_{dyn}(t-\tau)T'(\tau,r)d\tau - \lambda\Delta T(t,r) = \Phi(t,r), \quad (9)$$

where ρ and λ are the density and thermal conductivity of the material; $T'(t,r) = \frac{\partial}{\partial t}T(t,r)$, Δ—Laplacian, and $\Phi(t,r)$ are the volumetric heat flux density. Equation (9) has an analytical solution for a homogeneous boundary value problem. Assume that the dynamic heat capacity $c_{dyn}(t)$ is a completely monotonic function of time (this requirement is usually satisfied for glass-forming liquids [22]). Then, $c_{dyn}(t)$ can be represented by Equation (10)

$$c_{dyn}(t) = c_0 - (c_0 - c_{in})\int H(\tau_0)exp(-t/\tau_0)d\tau_0, \quad (10)$$

where $H(\tau_0)$ is the distribution function of the relaxation time τ_0; a c_{in} and c_0 are the initial and equilibrium heat capacities ($c_{dyn}(t) \to c_{in}$ as $t \to 0$, and $c_{dyn}(t) \to c_0$ as $t \to \infty$). To determine $H(\tau_0)$ for a particular material, broadband heat capacity spectroscopy can be used (for details, see [22]).

The solution of the boundary value problem for Equation (9) can be obtained in two stages. First, the problem is solved for the heat capacity $c_{dyn}(t)$ with Debye relaxation, shown in Equation (11),

$$c_{dyn}(t) = c_0[1 - \varepsilon_0 exp(-t/\tau_0)], \tag{11}$$

where $\varepsilon_0 = (c_0 - c_{in})/c_0$. After that, using the distribution function $H(\tau_0)$, the solution for a particular material can be obtained as a linear combination of solutions for different τ_0. Thus, Equation (12) follows on from Equations (9) and (11) for the heat capacity with Debye relaxation:

$$\frac{\partial}{\partial t}T(t,r) - D_0\Delta T(t,r) = \frac{\Phi(t,r)}{\rho c_0} + \varepsilon_0\frac{\partial}{\partial t}\int_0^t exp\left(-\frac{t-\tau}{\tau_0}\right)T'(t,r)d\tau, \tag{12}$$

where $D_0 = \lambda/\rho c_0$ is the equilibrium thermal diffusivity. The parameter ε_0 of various glass-forming liquids and polymers is usually in the range of 0.3–0.5 [53–56,61–63]. First, assume that a spherically symmetric heat source $\Phi(t,r) = \Phi(r)F(t)$ is distributed in a spherical volume of radius r_0. Next, consider the homogeneous boundary condition $T(t,R) = 0$ at a distance $R \gg r_0$ from the center of the heat source and the initial condition $T(t,r) = 0$ for $t \leq 0$. Then, Equation (13) is a solution to this boundary value problem.

$$T(t,r) = \sum_{n=1}\psi_n(t)\frac{sin(\pi nr/R)}{r}, \tag{13}$$

where $\psi_n(t)$ must satisfy Equation (14):

$$\psi_n'(t) + \frac{\psi_n(t)}{\tau_n} = \frac{r\Phi_n F(t)}{\rho c_0} + \varepsilon_0\frac{\partial}{\partial t}\int_0^t exp\left(-\frac{t-\tau}{\tau_0}\right)\psi_n'(\tau)d\tau, \tag{14}$$

where $\Phi_n = \frac{2}{R}\int_0^R r\Phi(r)sin(\pi nr/R)dr$ and $\tau_n^{-1} = D_0(\pi n/R)^2$. Here, let the heat flux be uniformly distributed in the volume of radius r_0 with volumetric density Φ_0. Then,

$$\Phi_n = 2R\Phi_0\frac{sin(\pi nr_0/R) - (\pi nr_0/R)\cdot cos(\pi nr_0/R)}{(\pi n)^2}. \tag{15}$$

For example, consider a sinusoidal heat flux with $F(t) = sin(2\pi t/\tau_p)$ for $t \in [0, \tau_p]$ and $F(t) = 0$ for $t \notin (0, \tau_p)$. Then, as follows from Equation (14), $\psi_n(t)$ are represented by Equation (16) and Equation (17) for $0 \leq t \leq \tau_p$ and $\tau_p < t$, respectively.

$$\psi_n(t) = \frac{\Phi_n}{\rho c_0}\frac{\tau_n\gamma_n\mu_n}{(\gamma_n-\mu_n)}\left[\frac{(\gamma_n\tau_0-1)\left[\gamma_n sin\left(2\pi t/\tau_p\right)+\frac{\pi m}{\tau_p}(exp(-\gamma_n t)-cos\left(2\pi t/\tau_p\right))\right]}{(\gamma_n)^2+\left(\frac{2\pi}{\tau_p}\right)^2} + \frac{(1-\mu_n\tau_0)\left[\mu_n sin\left(2\pi t/\tau_p\right)+\frac{2\pi}{\tau_p}(exp(-\mu_n t)-cos\left(2\pi t/\tau_p\right))\right]}{(\mu_n)^2+\left(\frac{2\pi}{\tau_p}\right)^2}\right], \tag{16}$$

$$\psi_n(t) = \frac{\Phi_n}{\rho c_0}\frac{2\pi\tau_n\gamma_n\mu_n}{\tau_p(\gamma_n-\mu_n)}\left[\frac{(\gamma_n\tau_0-1)\left[exp(-\gamma_n t)-exp(\gamma_n(\tau_p-t))\right]}{(\gamma_n)^2+\left(\frac{2\pi}{\tau_p}\right)^2} + \frac{(1-\mu_n\tau_0)\left[exp(-\mu_n t)-exp(\mu_n(\tau_p-t))\right]}{(\mu_n)^2+\left(\frac{2\pi}{\tau_p}\right)^2}\right], \tag{17}$$

where $-\gamma_n$ and $-\mu_n$ are equal to the roots of the polynomial $(1-\varepsilon_0)p^2 + p\left(\tau_n^{-1} + \tau_0^{-1}\right) + \tau_n^{-1}\tau_0^{-1}$. In addition, γ_n and μ_n are real and positive parameters; $\gamma_n - \mu_n \neq 0$ for $0 < \varepsilon_0 < 1$ and $0 < \tau_n, \tau_0$.

4. Local Thermal Perturbations during the Nucleation and Decay of Crystal Nuclei in Glass-Forming Liquids

To estimate the magnitude of the local temperature change $\delta T(t,r)$ during the nucleation in glass-forming liquids, we consider the nucleation of spherical crystalline nuclei. For a boundary value problem at $R \gg r_0$, the size of R is not significant. For example, we take $R = 300$ nm. Next, we consider the nucleation and decay of a nucleus with a subcritical radius r_0 of the order of 1 nm during $\tau_p = 1$ ns. The sinusoidal heat flux den-

sity $\Phi_0 \sin(2\pi t/\tau_p)$ can be considered as a simple model for the formation and decay of crystalline nuclei. The heat flux density required to compensate for the costs of nucleation is equal to $-\frac{\Delta g_v}{2} = -\frac{1}{2}\Delta h_m \Delta T/T_{m0}$. Therefore, $\Phi_0 = (-\pi \Delta h_m/2\tau_p)(\Delta T/T_{m0})$, since $\int_0^{\tau_p/2} \Phi_0 \sin(2\pi t/\tau_p)dt = \Phi_0 \tau_p/\pi$.

Consider, for example, the silicate glass $Na_2O{\cdot}2CaO{\cdot}3SiO_2$ with the thermal parameters given in Table 1. Thus, we take $\Delta T = 200$ K and use the parameters of this glass in the liquid phase [53,62–65]. Thus, the following parameters were used for model calculations: $\rho = 2.8$ g/cm^3, $\rho c_0 = 5 \times 10^6$ J/m^{3}K, $\lambda = 0.5$ W/m·K, $D_0 = 1 \times 10^{-7}$ m^2/s, $\varepsilon_0 = 1/2$, $T_{m0} = 1560$ K, $\Delta h_m = 7.2 \times 10^8$ J/m^3, and V_C = 292 nm^3. Let us consider nuclei close to the critical size. Then, at $r_0 = \sqrt[3]{3V_C/4\pi}$, we have r_0 = 4.1 nm. Then, $\delta T(t,r)$ can be calculated according to Equation (13) at various τ_0. For example, $\tau_0 = 0$, 0.1 ns, 1 ns, 10 ns, and 100 ns (see Figures 1 and 2). Note also that the sum of series (13) converges with the sum of series $1/n^2$. Therefore, to obtain a result with an accuracy of about 1%, it is enough to calculate the sum up to $N > 100$ terms, since the remainder of the sum is about $1/N$.

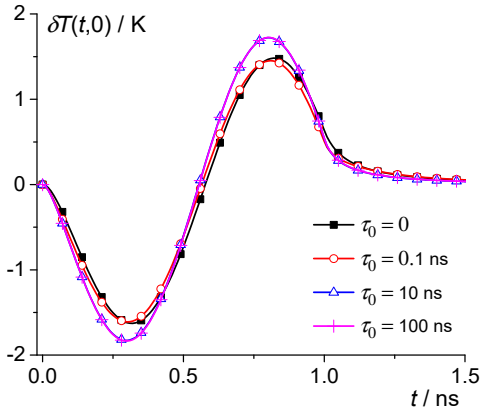

Figure 1. Dependence of the temperature change $\delta T(t,0)$ on time for the silicate glass $Na_2O{\cdot}2CaO{\cdot}3SiO_2$ at $\Delta T = 200$ K; $\tau_0 = 0$, 0.1 ns, 10 ns, and 100 ns—squares, circles, triangles, and crosses.

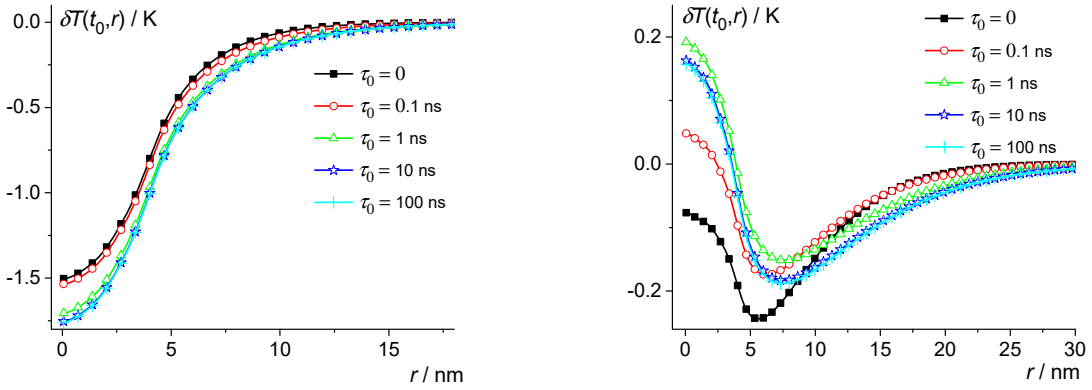

(**a**) (**b**)

Figure 2. Dependence of the temperature change $\delta T(t_0,r)$ on distance r at $t_0 = 0.25$ ns (**a**) and $t_0 = 0.57$ ns (**b**) for the silicate glass $Na_2O{\cdot}2CaO{\cdot}3SiO_2$ at $\Delta T = 200$ K; $\tau_0 = 0$, 0.1 ns, 1 ns, 10 ns, and 100 ns—squares, circles, triangles, stars, and crosses.

Thus, the magnitude of the local temperature change $\delta T(t,r)$ during the nucleation and decay of subcritical nuclei can reach about 1 K in silicate glass-forming liquids. The effect of dynamic heat capacity is significant at $\tau_0 = 10$ ns (see Figures 1 and 2). However,

at $\tau_0 = 0.1$ ns, this effect is small. The effect increases with τ_0 and reaches saturation when τ_0 approaches 10 ns (see Figure 2).

Similar results can be obtained for polymers (see Figures 3–6). Consider, for example, isotactic polystyrene (iPS) with the thermal parameters given in Table 3. Thus, we take $\Delta T = 30$ K and use the parameters of iPS in the liquid phase [13,54–56]. Thus, the following parameters were used for model calculations: $\rho = 1.05$ g/cm^3, $\rho c_0 = 1.8 \times 10^6$ J/m^{3}K, $\lambda = 0.14$ W/m·K, $D_0 = 0.8 \times 10^{-7}$ m^2/s, $\varepsilon_0 = 1/2$, $T_{m0} = 516$ K, $\Delta h_m = 0.91 \times 10^8$ J/m^3, and $V_C = 704.5$ nm^3. Let us consider nuclei close to the critical size. Then, at $r_0 = \sqrt[3]{3V_C/4\pi}$, we have $r_0 = 5.5$ nm. For example, we calculate $\delta T(t, r)$ using Equation (13) at $\tau_0 = 0$, 0.1 ns, 1 ns, 10 ns, and 100 ns, as well as when averaged over the distribution $H(\tau_0)$ (see Figures 3 and 4). The distribution $H(\tau_0)$ can be obtained from the broad band heat capacity spectroscopy (for details, see [22]). Moreover, relaxation phenomena in glass-forming materials can usually be described by the Kohlrausch relaxation function $exp\left(-(t/\tau_K)^\beta\right)$, where β is about 0.5. In addition,

$$H(\tau_0) = \frac{exp(-\tau_0/4\tau_K)}{\sqrt{4\pi\tau_K\tau_0}} \tag{18}$$

at $\beta = 0.5$ [66]. The Kohlrausch relaxation time $\tau_K(T)$ can be obtained from the Vogel–Fulcher–Tammann–Hesse (VFTH) equation

$$\log(\omega_{max}(T)) = A - B/(T - T_0). \tag{19}$$

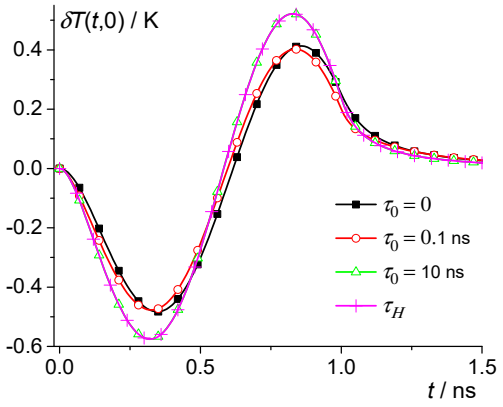

Figure 3. Dependence of the temperature change $\delta T(t, 0)$ on time for iPS at $\Delta T = 30$ K. $\tau_0 = 0$, 0.1 ns, and 10 ns—squares, circles, and triangles; crosses are the result of averaging δT over the distribution $H(\tau_0)$.

The parameters of this equation can be measured using broad band heat capacity spectroscopy [21]. In fact, $\tau_K(T)$ is inversely proportional to the frequency $\omega_{max}(T)$, which corresponds to the maximum of the imaginary part of the dynamic heat capacity (see [22]). For polystyrene, $A = 10.2$, $B = 388$ K, and $T_0 = 341.5$ K [21]. Thus, we obtain the Kohlrausch relaxation time τ_K and the distribution function $H(\tau_0)$ at different temperatures from the VFTH equation. However, the profile of the distribution function $H(\tau_0)$ is not very important, because the influence of the dynamic heat capacity reaches saturation at τ_0 of the order of tens of ns (see Figure 4).

Thus, the magnitude of the local temperature change $\delta T(t,r)$ during the nucleation in iPS is about 0.5 K (a similar result was obtained for PE). The effect of dynamic heat capacity reaches saturation at $\tau_0 > 10$ ns (see Figures 3 and 4). As a consequence, $\delta T(t, r)$ at $\tau_0 = 10$ ns and 100 ns are practically the same and coincide with the result of averaging over the distribution $H(\tau_0)$ (see Figures 3 and 4). Thus, the effect of dynamic heat capacity is significant on the nanosecond time scale. It should be noted that due to the dynamic heat

capacity, thermal perturbations $\delta T(t_0, r)$ at $\tau_0 > 0.1$ ns and $\tau_0 = 0$ even have opposite signs at $t_0 = 0.6$ ns and $r < 5$ nm (see Figure 4b).

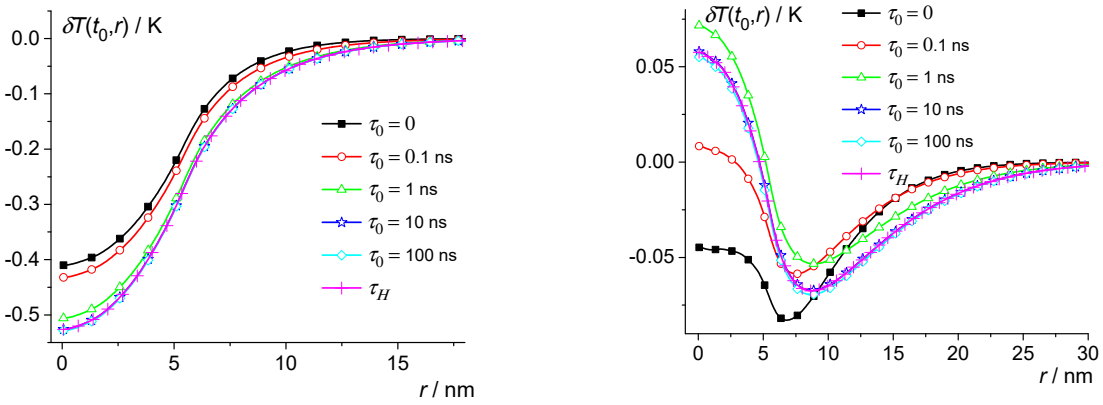

(**a**) (**b**)

Figure 4. Dependence of the temperature change $\delta T(t_0, r)$ on distance r at $t_0 = 0.25$ ns (**a**) and $t_0 = 0.6$ ns (**b**) for iPS at $\Delta T = 30$ K. $\tau_0 = 0$, 0.1 ns, 1 ns, 10 ns, and 100 ns—squares, circles, triangles, stars, and diamonds; crosses are the result of averaging δT over the distribution $H(\tau_0)$.

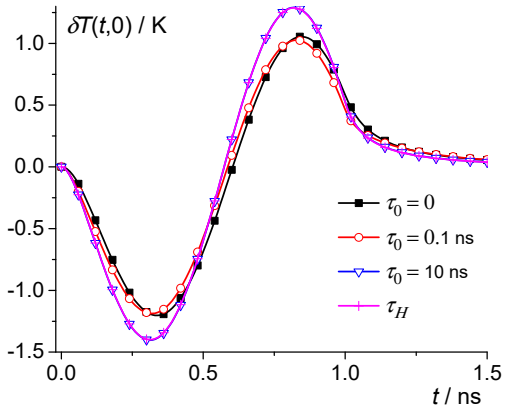

Figure 5. Dependence of the temperature change $\delta T(t, 0)$ on time for PBS at $\Delta T = 60$ K. $\tau_0 = 0$, 0.1 ns, and 10 ns—squares, circles, and triangles; crosses are the result of averaging δT over the distribution $H(\tau_0)$.

A larger local temperature change $\delta T(t,r)$ can be estimated for the biodegradable polymer polybutylene succinate (PBS) (see Table 4). For example, we take $\Delta T = 60$ K and use the parameters of polybutylene succinate in the liquid phase [54–60]. For model calculations, we use the following parameters: $\rho = 1.26$ g/cm^3, $\rho c_0 = 2.4 \times 10^6$ J/m^{3}K, $\lambda = 0.09$ W/m·K, $D_0 = 0.4 \times 10^{-7}$ m^2/s, $\varepsilon_0 = 1/2$, $T_{m0} = 403$ K, $\Delta h_m = 1.47 \times 10^8$ J/m^3, and $V_C = 152.6$ nm^3, and consider nuclei close to the critical size. Then, at $r_0 = \sqrt[3]{3V_C/4\pi}$, we have $r_0 = 3.3$ nm. The distribution function $H(\tau_0)$ for PBS at different temperatures can be obtained from dielectric spectroscopy data using the parameters ($A = 9.5$, $B = 526.3$ K, and $T_0 = 218.2$ K) of the VFTH equation [67].

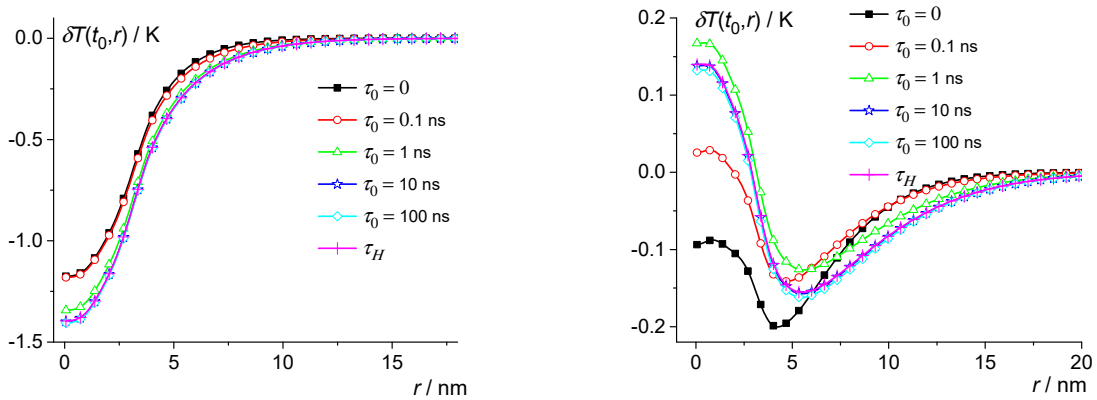

Figure 6. Dependence of the temperature change $\delta T(t_0, r)$ on distance r at $t_0 = 0.3$ ns (**a**) and $t_0 = 0.59$ ns (**b**) for PBS at $\Delta T = 60$ K. $\tau_0 = 0$, 0.1 ns, 1 ns, 10 ns and 100 ns—squares, circles, triangles, stars, and diamonds; crosses are the result of averaging δT over the distribution $H(\tau_0)$.

The magnitude of the local temperature change $\delta T(t, r)$ during the nucleation in PBS is about 1 K (see Figures 5 and 6) (a similar result was obtained for iPP). The effect of dynamic heat capacity reaches saturation when τ_0 increases above tens of ns. As a result, the profile of the distribution function $H(\tau_0)$ is not very important (see Figures 4 and 6).

The relative change in the rate of nucleation $\frac{I(T+\delta T)}{I(T)}$ depends on the value of δT, which in turn, depends on the dynamic heat capacity of the glass-forming liquid. Let us denote by δT^* and δT the temperature perturbations with and without the influence of the dynamic heat capacity, respectively. In fact, δT^* is approximately 20–30% greater than δT (see Figures 1 and 6). As a result, $\frac{I(T+\delta T^*)}{I(T)}$ is an order of magnitude larger than $\frac{I(T+\delta T)}{I(T)}$. For example, in polybutylene succinate, $\frac{\Delta G_C}{k_B T} = 354$ at $\Delta T = 60$ K (see Table 4) and $(\delta T^* - \delta T)$ is about 0.25 K at t of about 0.25–0.3 ns (see Figures 4 and 5). Therefore, the ratio $\frac{I(T+\delta T^*)}{I(T+\delta T)} = \exp\left(-\frac{\Delta G_C}{k_B T} \cdot \frac{2(\delta T^* - \delta T)}{\Delta T}\right)$ is about 20. Thus, the change in the nucleation rate is significantly enhanced due to the influence of the dynamic heat capacity $c_{dyn}(t)$ of glass-forming liquids.

5. Conclusions

The development of new advanced materials with artificial nanostructures requires a deep understanding of the thermal processes during the nucleation of crystals in glass-forming substances and polymers. We found that local temperature changes associated with the energy required for the formation of crystal nuclei in glass-forming liquids can be of the order of 1 K, which can significantly change the evolution of near-critical nuclei and the dynamics of nucleation. In fact, a significant number of subcritical nuclei can become stable, since the critical radius and the energy barrier ΔG_C decrease with decreasing local temperature, due to local energy costs for the formation of a nucleus. Local temperature perturbations during crystal nucleation in silicate glasses and polymers have been found to change the nucleation rate by 2–5 orders of magnitude. Moreover, the change in the nucleation rate is enhanced by an order of magnitude, due to the effect of the dynamic heat capacity $c_{dyn}(t)$ of glass-forming liquids. The effect of the dynamic heat capacity $c_{dyn}(t)$ on local thermal perturbations in glass-forming liquids can be described by an integro-differential heat equation with "memory". This equation can be solved analytically for a spherically symmetric problem. It has been established that even fast (about 1 ns) components of the dynamic heat capacity $c_{dyn}(t)$ significantly enhance local temperature perturbations arising during nucleation in glass-forming liquids. This effect is enhanced with an increase in the relaxation time τ_0 of the dynamic heat capacity $c_{dyn}(t)$. The influ-

ence of $c_{dyn}(t)$ saturates as τ_0 increases above tens of ns. This study can be helpful for understanding the processes of nanocrystallization in glass-forming liquids and for the technology of nanostructured glasses, polymers, and composites.

Author Contributions: Conceptualization, A.M.; formal analysis, A.M.; methodology, A.M.; supervision, C.S.; visualization, A.M.; writing—original draft, A.M.; writing—review and editing, C.S. All authors have read and agreed to the published version of the manuscript.

Funding: This research received no external funding.

Data Availability Statement: The datasets generated during and/or analyzed during the current study are available from the corresponding author on reasonable request.

Acknowledgments: A.M. acknowledges the administrative and technical support of the Prokhorov General Physics Institute of the Russian Academy of Sciences.

Conflicts of Interest: The authors declare no conflict of interest.

Nomenclature

Latin Symbols

A	parameter of the VFTH equation (dimensionless)
B and T_0	parameters of the VFTH equation (K)
c_{in}, c_0	initial and equilibrium heat capacities ($J{\cdot}kg^{-1}{\cdot}K^{-1}$)
$c_{dyn}(t)$	dynamic heat capacity ($J{\cdot}kg^{-1}{\cdot}K^{-1}$)
D_0	equilibrium thermal diffusivity ($m^2{\cdot}s^{-1}$)
E_A	activation energy for the transport of segments in polymers ($kJ{\cdot}mol^{-1}$)
ΔG_D	kinetic barrier to nucleation (J)
ΔG_C	energy barrier for homogeneous nucleation (J)
Δg_v	change in volumetric Gibbs free energy at crystallization ($J{\cdot}m^{-3}$)
Δh_m	volumetric enthalpy of melting ($J{\cdot}m^{-3}$)
$H(\tau_0)$	distribution function (s^{-1})
$I(T)$	nucleation rate ($m^{-3}{\cdot}s^{-1}$)
k_B	Boltzmann constant ($J{\cdot}K^{-1}$)
l_C	critical lateral thickness (nm)
R	universal gas constant ($J{\cdot}mol^{-1}{\cdot}K^{-1}$)
R_{min}	minimum work needed to form the nucleus (J)
r_C	critical radius (nm)
δT	local change in temperature (K)
ΔT	undercooling (K)
T_g	glass transition temperature (K)
T_{m0}	equilibrium melting temperature (K)
V_C	volume of the critical nucleus (nm^3)
V_{sound}	sound speed ($m{\cdot}s^{-1}$)

Greek Symbols

γ_n	relaxation parameter (dimensionless)
ε_0	coefficient $\varepsilon_0 = (c_0 - c_{in})/c_0$ (dimensionless)
η	viscosity (Pa·s)
λ	thermal conductivity ($W{\cdot}m^{-1}{\cdot}K^{-1}$)
μ_n	relaxation parameter (dimensionless)
ρ	density ($kg{\cdot}m^{-3}$)
σ	interfacial free energy ($J{\cdot}m^{-2}$)
σ_e	interfacial free energy for fold surface ($J{\cdot}m^{-2}$)
τ_0	Debye relaxation time (s)
τ_K	Kohlrausch relaxation time (s)
τ_n	relaxation time (s)
τ_p	time of nucleation and decay of a subcritical nucleus (s)

$\Phi(t,r)$	volumetric heat flux density (W·m^{-3})
Φ_0	volumetric heat flux density (W·m^{-3})
Φ_n	nth Fourier component (W·m^{-2})
$\psi_n(t)$	nth Fourier component (K·m)
ω	temperature modulation frequency (rad·s^{-1})

References

1. Liu, H.; Jiang, Q.; Huo, J.; Zhang, Y.; Yang, W.; Li, X. Crystallization in additive manufacturing of metallic glasses: A review. *Addit. Manuf.* **2020**, *36*, 101568. [CrossRef]
2. Li, X.P. Additive manufacturing of advanced multi-component alloys: Bulk metallic glasses and high entropy alloys. *Adv. Eng. Mater.* **2018**, *20*, 1700874. [CrossRef]
3. Liu, H.; Yang, D.; Jiang, Q.; Jiang, Y.; Yang, W.; Liu, L.; Zhang, L.C. Additive manufacturing of metallic glasses and high-entropy alloys: Significance, unsettled issues, and future directions. *J. Mat. Sci. Technol.* **2022**, *140*, 79–120. [CrossRef]
4. Zhang, Y.; Liu, H.; Mo, J.; Wang, M.; Chen, Z.; He, Y.; Yang, W.; Tang, C. Atomic-level crystallization in selective laser melting fabricated Zr-based metallic glasses. *Phys. Chem. Chem. Phys.* **2019**, *21*, 12406–12413. [CrossRef]
5. Perepezko, J.H.; Gao, M.; Wang, J.Q. Nanoglass and nanocrystallization reactions in metallic glasses. *Front. Mater.* **2021**, *8*, 663862. [CrossRef]
6. Zhao, B.; Yang, B.; Abyzov, A.S.; Schmelzer, J.W.P.; Rodríguez-Viejo, J.; Zhai, Q.; Schick, C.; Gao, Y. Beating homogeneous nucleation and tuning atomic ordering in glass-forming metals by nanocalorimetry. *Nano Lett.* **2017**, *17*, 7751–7760. [CrossRef]
7. Wang, L.; Ma, L.; Kimura, H.; Inoue, A. Amorphous Forming Ability and Mechanical Properties of Rapidly Solidified Al–Zr–LTM (LTM=Fe, Co, Ni and Cu) Alloys. *Mater. Lett.* **2002**, *52*, 47–52. Available online: https://www.sciencedirect.com/journal/materials-letters/vol/52/issue/1 (accessed on 23 November 2022). [CrossRef]
8. Mansouri, M.; Simchi, A.; Varahram, N.; Park, E.S. Development of fcc-Al nanoparticles during crystallization of amorphous Al–Ni alloys containing mischmetal: Microstructure and hardness evaluation. *Mater. Sci. Eng. A* **2014**, *604*, 92–97. [CrossRef]
9. Singh, D.; Singh, D.; Mandal, R.K.; Srivastava, O.N.; Tiwari, R.S. Crystallization behavior and mechanical properties of (Al90Fe5Ce5)100−xTix amorphous alloys. *J. Alloys Comp.* **2016**, *687*, 990–998. [CrossRef]
10. Lee, B.S.; Burr, G.W.; Shelby, R.M.; Raoux, S.; Rettner, C.T.; Bogle, S.N.; Darmawikarta, K.; Bishop, S.G.; Abelson, J.R. Observation of the role of subcritical nuclei in crystallization of a glassy solid. *Science* **2009**, *326*, 980–984. [CrossRef] [PubMed]
11. Orava, J.; Greer, A.L. Fast crystal growth in glass-forming liquids. *J. Non Crystal. Sol.* **2016**, *451*, 94–100. [CrossRef]
12. Fokin, V.M.; Zanotto, E.D.; Yuritsyn, N.S.; Schmelzer, J.W.P. Homogeneous crystal nucleation in silicate glasses: A 40 years perspective. *J. Non-Crystal. Sol.* **2006**, *352*, 2681–2714. [CrossRef]
13. Hoffman, J.D.; Davis, G.T.; Lauritzen, J.I., Jr. The rate of crystallization of linear polymers with chain folding. In *Treatise on Solid State Chemistry*; Hannay, N.B., Ed.; Springer: Boston, MA, USA, 1976. [CrossRef]
14. Andrianov, R.A.; Androsch, R.; Zhang, R.; Mukhametzyanov, T.A.; Abyzov, A.S.; Schmelzer, J.W.P.; Schick, C. Growth and dissolution of crystal nuclei in poly(l-lactic acid) (PLLA) in Tammann's development method. *Polymer* **2020**, *196*, 122453. [CrossRef]
15. Schick, C.; Androsch, R.; Schmelzer, J.W.P. Homogeneous crystal nucleation in polymers. *J. Phys. Condens. Matter.* **2017**, *29*, 453002. [CrossRef]
16. Reiter, G.; Strobl, G.R. *Progress in Understanding of Polymer Crystallization, Lecture Notes in Physics*; Springer: Berlin/Heidelberg, Germany, 2007; ISBN 10: 9783540473053. [CrossRef]
17. Russo, J.; Tanaka, H. The microscopic pathway to crystallization in supercooled liquids. *Sci. Rep.* **2012**, *2*, 505. [CrossRef]
18. Wyslouzil, B.E.; Seinfeld, J.H. Nonisothermal homogeneous nucleation. *J. Chem. Phys.* **1992**, *97*, 2661–2670. [CrossRef]
19. Birge, N.O.; Nagel, S.R. Specific heat spectroscopy of the glass transition. *Phys. Rev. Lett.* **1985**, *54*, 2674–2677. [CrossRef] [PubMed]
20. Korus, J.; Beiner, M.; Busse, K.; Kahle, S.; Unger, R.D. Heat capacity spectroscopy at the glass transition in polymers. *Thermochim. Acta* **1997**, *304–305*, 99–110. [CrossRef]
21. Chua, Y.Z.; Schulz, G.; Shoifet, E.; Huth, H.; Zorn, R.; Scmelzer, J.W.P.; Schick, C. Glass transition cooperativity from broad band heat capacity spectroscopy. *Colloid Polym. Sci.* **2014**, *292*, 1893–1904. [CrossRef]
22. Minakov, A.; Schick, C. Nanometer scale thermal response of polymers to fast thermal perturbations. *J. Chem. Phys.* **2018**, *149*, 074503. [CrossRef]
23. Landau, L.D.; Lifshitz, E.M. *Course of Theoretical Physics 5: Statistical*, 3rd ed.; Butterworth-Heinemann: Oxford, UK, 1980; ISBN 13: 978-0750633727.
24. Landau, L.D.; Lifshitz, E.M. *Course of Theoretical Physics 10: Physical Kinetics*, 1st ed.; Pergamon Press: Oxford, UK; Frankfurt, Germany, 1981; ISBN 978-0-08-026480-6.
25. Schmelzer, J.W.P. Application of the Nucleation Theorem to Crystallization of Liquids: Some General Theoretical Results. *Entropy* **2019**, *21*, 1147. [CrossRef]
26. Kelton, K.F.; Greer, A.L. Nucleation in Condensed Matter—Applications in Materials and Biology. *Pergamon Mater. Ser.* **2010**, *15*, 1–15. [CrossRef]
27. Kashchiev, D.; van Rosmalen, G.M. Review: Nucleation in solutions revisited. *Cryst. Res. Technol.* **2003**, *38*, 555–574. [CrossRef]

28. Lide, D.R. *CRC Handbook of Chemistry and Physics*, 90th ed.; CRC Press: Boca Raton, FL, USA, 2010; ISBN 13: 978-1420090840/10:1420090844.
29. Minakov, A.A.; Schick, C. Integro-differential equation for the non-equilibrium thermal response of glass-forming materials: Analytical solutions. *Symmetry* **2021**, *13*, 256. [CrossRef]
30. Blow, K.E.; Quigley, D.; Sosso, G.C. The seven deadly sins: When computing crystal nucleation rates, the devil is in the details. *J. Chem. Phys.* **2021**, *155*, 040901. [CrossRef] [PubMed]
31. Separdar, L.; Rino, J.P.; Zanotto, E.D. Unveiling nucleation dynamics by seeded and spontaneous crystallization in supercooled liquids. *Comput. Mater. Sci.* **2021**, *199*, 110802. [CrossRef]
32. Tipeev, A.O.; Zanotto, E.D.; Rino, J.P. Crystal nucleation kinetics in supercooled germanium: MD simulations versus experimental data. *J. Phys. Chem. B* **2020**, *124*, 7979–7988. [CrossRef] [PubMed]
33. Mahata, A.; Zaeem, M.A.; Baskes, M.I. Understanding homogeneous nucleation in solidification of aluminum by molecular dynamics simulations. *Model. Simul. Mater. Sci. Eng.* **2018**, *26*, 025007. [CrossRef]
34. Fitzner, M.; Sosso, G.C.; Coxa, S.J. Michaelidesa, Ice is born in low-mobility regions of supercooled liquid water. *Proc. Natl. Acad. Sci. USA* **2019**, *116*, 2009–2014. [CrossRef] [PubMed]
35. Sosso, G.C.; Miceli, G.; Caravati, S.; Giberti, F.; Behler, J.; Bernasconi, M. Fast Crystallization of the Phase Change Compound GeTe by Large-Scale Molecular Dynamics Simulations. *J. Phys. Chem. Lett.* **2013**, *4*, 4241–4246. [CrossRef]
36. Sosso, G.C.; Chen, J.; Cox, S.J.; Fitzner, M.; Pedevilla, P.; Zen, A.; Michaelides, A. Crystal Nucleation in Liquids: Open Questions and Future Challenges in Molecular Dynamics Simulations. *Chem. Rev.* **2016**, *116*, 7078–7116. [CrossRef] [PubMed]
37. Lee, B.M.; Baik, H.K.; Seong, B.S.; Munetoh, S.; Motooka, T. Molecular-dynamics analysis of the nucleation and crystallization process of Si. *Phys. B Condens. Matter* **2007**, *392*, 266–271. [CrossRef]
38. Sanz, E.; Vega, C.; Espinosa, J.R.; Caballero-Bernal, R.; Abascal, J.L.F.; Valeriani, C. Homogeneous Ice Nucleation at Moderate Supercooling from Molecular Simulation. *J. Am. Chem. Soc.* **2013**, *135*, 15008–15017. [CrossRef] [PubMed]
39. Zhang, Z.; Yang, X. The effect of chain interpenetration on an ordering process in the early stage of polymer crystal nucleation. *Polymer* **2006**, *47*, 5213–5219. [CrossRef]
40. Yamamoto, T. Molecular dynamics simulation of polymer crystallization through chain folding. *J. Chem. Phys.* **1997**, *107*, 2653–2663. [CrossRef]
41. Waheed, N.; Ko, M.J.; Rutledge, G.C. Molecular simulation of crystal growth in long alkanes. *Polymer* **2005**, *46*, 8689–8702. [CrossRef]
42. Gu, J.; Wang, X.; Wu, J.; Wang, X. Molecular Dynamics Simulation of Chain Folding for Polyethylene Subjected to Vibration Excitation. *Int. J. Polym. Sci.* **2014**, *2014*, 506793. [CrossRef]
43. Luo, C.; Sommer, J.U. Frozen topology: Entanglements control nucleation and crystallization in polymers. *Phys. Rev. Lett.* **2014**, *112*, 195702. [CrossRef]
44. Kelton, K.F. Crystal nucleation in liquids and glasses. *Solid State Phys.* **1991**, *45*, 75–177. [CrossRef]
45. Rodrigues, L.R.; Fokin, A.S.A.V.M.; Zanotto, E.D. Effect of structural relaxation on crystal nucleation in a soda-lime-silica glass. *J. Am. Ceram. Soc.* **2021**, *104*, 3212–3223. [CrossRef]
46. Schmelzer, J.W.P.; Tropin, T.V.; Fokin, V.M.; Abyzov, A.S.; Zanotto, E.D. Effects of Glass Transition and Structural Relaxation on Crystal Nucleation: Theoretical Description and Model Analysis. *Entropy* **2020**, *22*, 1098. [CrossRef]
47. Rodrigues, L.R.; Abyzov, A.S.; Fokin, V.M.; Schmelzer, J.W.P.; Zanotto, E.D. Relaxation effect on crystal nucleation in a glass unveiled by experimental, numerical, and analytical approaches. *Acta Mater.* **2022**, *223*, 117458. [CrossRef]
48. Schmelzer, J.W.P.; Tropin, T.V. Theory of crystal nucleation of glass-forming liquids: Some new developments. *Int. J. Appl. Glass Sci.* **2022**, *13*, 171–198. [CrossRef]
49. Cabral, A.A.; Fokin, V.M.; Zanotto, E.D. Nanocrystallization of fresnoite glass. II. Analysis of homogeneous nucleation kinetics. *J. Non Crystal. Sol.* **2004**, *343*, 85–90. [CrossRef]
50. Zanotto, E.D.; Fokin, V.M. Recent Studies of Internal and Surface Nucleation In Silicate Glasses. *Phil. Trans. R. Soc. Lond. A* **2003**, *361*, 591–613. [CrossRef]
51. Granasy, L.; Igioi, F. Comparison of experiments and modern theories of crystal nucleation. *J. Chem. Phys.* **1997**, *107*, 3634. Available online: https://aip.scitation.org/doi/10.1063/1.474721 (accessed on 23 November 2022). [CrossRef]
52. Zanotto, E.D.; Weinberg, M. Trends in homogeneous crystal nucleation in oxide glasses. *Phys. Chem. Glasses Eur. J. Glass Sci. Technol. Part B* **1989**, *30*, 186–192.
53. Gonzalez-Oliver, C.J.R.; James, P.F. Crystal nucleation and growth in a $Na_2O_2CaO_3SiO_2$ glass. *J. Non Crystal. Sol.* **1980**, *38–39*, 699–704. [CrossRef]
54. van Krevelen, D.W.; Nijenhuis, K.T. *Properties of Polymers*, 4th ed.; Elsevier Science: Amsterdam, The Netherlands, 2009; ISBN 978-0-08-054819-7.
55. Mark, J.E. *Polymer Data Handbook*, 2nd ed.; Oxford University Press: Oxford, UK, 2009; ISBN 13: 978-0195181012/10:0195181018.
56. Mark, J.E. *Physical Properties of Polymers Handbook*; Springer: New York, NY, USA, 2007; ISBN 978-0-387-31235-4.
57. Qiu, Z.; Yang, W. Crystallization kinetics and morphology of poly(butylene succinate)/poly(vinyl phenol) blend. *Polymer* **2006**, *47*, 6429–6437. [CrossRef]
58. Deng, Y.; Thomas, N.L. Blending poly(butylene succinate) with poly(lactic acid): Ductility and phase inversion effects. *Eur. Polym. J.* **2015**, *71*, 534–546. [CrossRef]

59. Schick, C.; Toda, A.; Androsch, R. The narrow thickness distribution of lamellae of poly(butylene succinate) formed at low melt supercooling. *Macromolecules* **2021**, *54*, 3366–3376. [CrossRef]
60. Saffian, H.A.; Yamaguchi, M.; Ariffin, H.; Abdan, K.; Kassim, N.K.; Lee, S.H.; Lee, C.H.; Shafi, A.R.; Alias, A.H. Thermal, Physical and Mechanical Properties of Poly(Butylene Succinate)/Kenaf Core Fibers Composites Reinforced with Esterified Lignin. *Polymers* **2021**, *13*, 2359. [CrossRef] [PubMed]
61. Huang, J.; Gupta, P.K. Temperature dependence of the isostructural heat capacity of a soda lime silicate glass. *J. Non Crystal. Sol.* **1992**, *139*, 239–247. [CrossRef]
62. Stebbins, J.F.; Carmichael, I.S.E.; Moret, L.K. Heat capacities and entropies of silicate liquids and glasses. *Contrib. Mineral. Petrol.* **1984**, *86*, 131–148. [CrossRef]
63. Hofmeister, A.M.; Sehlke, A.; Avard, G.; Bollasina, A.J.; Robert, G.; Whittington, A.G. Transport properties of glassy and molten lavas as a function of temperature and composition. *J. Volcanol. Geotherm. Res.* **2016**, *327*, 330–348. [CrossRef]
64. Kang, Y.; Lee, J.; Morita, K. Thermal Conductivity of Molten Slags: A Review of Measurement, Techniques and Discussion Based on Microstructural Analysis. *ISIJ Int.* **2014**, *54*, 2008–2016. [CrossRef]
65. Sukenaga, S.; Endo, T.; Nishi, T.; Yamada, H.; Ohara, K.; Wakihara, T.; Inoue, K.; Kawanishi, S.; Ohta, H.; Shibata, H. Thermal Conductivity of Sodium Silicate Glasses and Melts: Contribution of Diffusive and Propagative Vibration Modes. *Front. Mater.* **2021**, *8*, 753746. [CrossRef]
66. Berberan-Santos, M.N.; Bodunov, E.N.; Valeur, B. Mathematical functions for the analysis of luminescence decays with underlying distributions 1 Kohlrausch decay function (stretched exponential). *Chem. Phys.* **2005**, *315*, 171–182. [CrossRef]
67. Ezzeddine, I.; Ghorbel, N.; Ilsouk, M.; Arous, M.; Lahcini, M.; Bouharras, F.Z.; Raihane, M.; Kallel, A. Dielectric and thermal characteristics of Beidellite nanoclay-reinforced poly (butylene succinate). *Mater. Chem. Phys.* **2021**, *258*, 123855. [CrossRef]